GROUND'2016
&
7th LPE

International Conference on Grounding and Earthing
&
7th International Conference on Lightning Physics and Effects

Porto de Galinhas, Brazil June, 2016

FIRST ANALYSIS OF ELECTRIC FIELD MILL NETWORK MEASUREMENTS FROM 2013 TO 2015.

Moacir Lacerda[1], Luana Feitosa[1,2], Oniel Rodrigues Silvestre[1] , Andressa Duarte[1,2], Clovis Lasta Fritzen[1], Waldeir Moreschi Dias[1] , Robson Jaques Verly [3]
[1] Laboratory of Atmospheric Sciences (LCA), Physics Institute (INFI), Federal University of Mato Grosso do Sul.
[2]Faculdade de Engenharia, Federal University of Mato Grosso do Sul.
[3] Instituto Federal do Mato Grosso, Campus Primavera do Leste

Abstract - In this paper we present details of construction and calibration of an Electric Field Mill (EFM) and first results of data analysis collected between 2013 and 2015 of an EFM network installed in the city of Campo Grande, Mato Grosso do Sul, Brazil and operated by the Laboratory of Atmospheric Sciences of the Physics Institute from the Federal University of Mato Grosso do Sul (www.lca.ufms.br). We present data analysis of 21 storms and fair weather measurements. We detected some patterns of previous discharges inside clouds that allow giving some insights of how to obtain an alert of lightning risk. The end of storm (EOS) was analyzed too. The fair weather electric field was analyzed by using Fourier Transform and allowed to detect the frequency of several harmonics. We used the first 21 harmonics to fit the data curve. The main oscillation has a period of about 12 hours. The system was monitored by cameras and we could synchronize the electric field measurement with video image. Some images of lightning discharge are showed. Some details of the sensors calibrating are presented.

1. - INTRODUCTION

Monitoring storms with an EFM network is an old, useful technique to prevent risks of damages and injuries to structures and people [1], [2]. False alerts and no alert are possibly related to the characteristic of the EFM network and the distance of cloud. Another kind of study is detect the charge structure inside clouds. Lacerda et al studied lightning activity over the city of São Paulo, Brazil, using EFM network and radar, and detected the positions of charge centers using the Inverse Problem of Coulomb's Law [3]. With the purpose of studying both fair weather and thunderstorm electric field, we have built the electric field sensors and installed an EFM network in the city of Campo Grande, Mato Grosso do Sul, Brazil, since 2013. The region was monitored with a system of four video cameras that were synchronized with the EFM network. The network is showed in Figure 1(a) and typical data are shown in Figures 5, 10, 11 and 12.

2. – NETWORK

The figure 1a shows one of this EFM network configurations during this period. The three main sensors used in this paper are: 002-INFI (lat -20.503323 long -54.611245); 006-Quimica_UFMS (lat -20.505078 long -54.617705); 007-Waldeir (lat -20.5332943; long -54.644605).

The sensors were developed and calibrated by the Laboratory of Atmospheric Sciences. The Figure 1b shows the electronic circuit, and figure 1c, shows a typical installation of the sensor.

The sensor requires only an electrical connection for power supply. If it's necessary, in a remote installation, can be used a photovoltaic plate and a battery.

The sensor's data and location are transmitted by a radio transmitter and do not require any cable. The signal reception is made by a receiver connected in an USB computer port. The data files are saved in a computer and uploaded to a site that processes them and builds graphical figures as shown in Figures 1a, 5, 10, 11 and 12.

We successfully developed a version of EFM that uses Raspberry Pi™ (RPi) plates coupled to the radio receiver that bypass the requirement of a computer. It improved substantially the applications of the sensor due to the low price, size, discrete appearance and features of RPi that includes 4 USB ports, 40 GPIO pins, Ethernet port, Combined 3.5mm audio jack and composite video, Camera interface (CSI), Display interface (DSI), Micro SD card slot, VideoCore IV 3D graphics core.

(a)

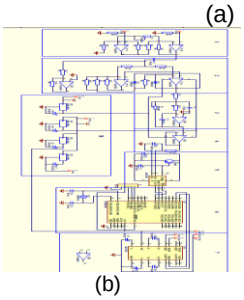

(b)

(c)

Figure 1(a) EFM Network (initial configuration) (b) - Electronic circuit of EFM. (Numeration from top to bottom) 1- Signal Amplifier; 2- Rectifier; 3- Filter; 4- Buffer; 5- Convertor AD; 6- Microcontroller; 7- Conversor TTL / RS232; 8- Source of power. There is a Module GPS ME-1000Rw or Garmin gps18x lvs, not represented in this diagram (c). Typical installation of sensor

3. – TYPICAL RESULTS

In this section we show results of both systems installed: The video cameras and the EFM network.

3.1 – VIDEO IMAGES

The cameras are installed over a 45 m metallic tower and cover the four directions (roughly N, S, E, W). They are numbered from 1 to 4 and can detect the luminosity of lightning strikes at height of 10 km about 300 km far from the tower. In Figure 2 we show a typical video image: camera 3 detects lightning activity and Ccmera 4 is out of focus. They can be used to direct high speed camera during thunderstorms.

Figure 2 Typical video image (four cameras) 12/01/2015, 23:45:13 UTC, Position of Camera 1: top-left, 2: top-right, 3: down-left and 4: down-right.

3.2 - ELECTRIC FIELD MEASUREMENT

3.2.1 CALIBRATION OF ELECTRIC FIELD MILL

The electrical scheme for calibrating the EFM is presented in figure 3. The applied electrical field, E =ΔVa / d, produces a lecture ΔVb, which is used to obtain the fit of figure 4.

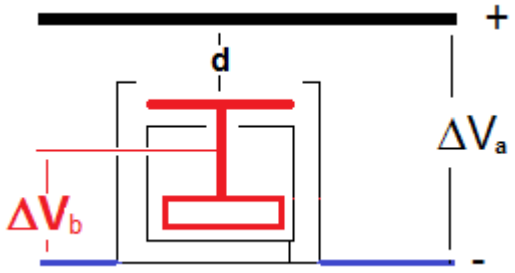

Figure 3. Electrical scheme for calibrating the EFM. The isolated sensor is in red. The thin black lines represent the metallic case. The black line over represents the positive metallic plate. The blue lines are the negative cable.

The calibration was made with a metallic plate over the sensor at a distance d = 2,5 cm in which a voltage drop, ΔVa, was applied from -230 V to +230V with steps of +5 V which corresponds to apply electric field from -9200 V/m to 9200 V/m with steps of 200 V/m.

The range of measurement voltage, ΔVb, of the electric circuit shown in figure 1b is from -4000V to +4000V. So, figure 3 shows the linear fit used to calibrate the sensor. Notice that the range of calibrations correspond to the linear behavior of the sensor. The R2 is 0,997. For increasing the range of measurements, when necessary, we use a polynomial fit of order 3. The equation of fitting data is then recorded in the integrated circuit to the firmware. It is important to speak about electric field sign convention in this research. Based on the calibration process, we have positive electric field when there is a positively charged plate over the sensor. Using this calibration to atmospheric fair weather situation, we notice that in this study the fair weather is considered positive (contrary to usual convention, where fair weather is negative, pointing downward). This is equivalent to say, in terms of convention, that our positive axis is pointing downward.

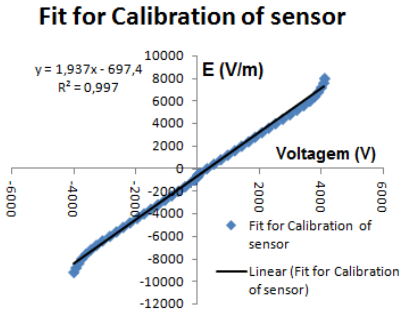

Figure 4. Sensor Calibration. Axis y represents E =ΔVa / d and axis x, ΔVb (see figure 3).

3.2.2 TYPICAL MEASUREMENT OF ELECTRIC FIELD

The Figure 5 shows the thunderstorm data recorded simultaneously by 3 sensors, among those showed in Figure 1a. This event presents two advantages of using EFM network. The first one is to record weak local meteorological storms with lightning activity. The second advantage of multiple sensor networks is to increase the effectiveness of alert better then when using only a threshold to electric field with a single sensor. . Notice that the values in figure 4 of one sensor (FAMEZ) is lower then the others. Only one is greater than 500 V/m that could be a possible reference for emitting an alert.

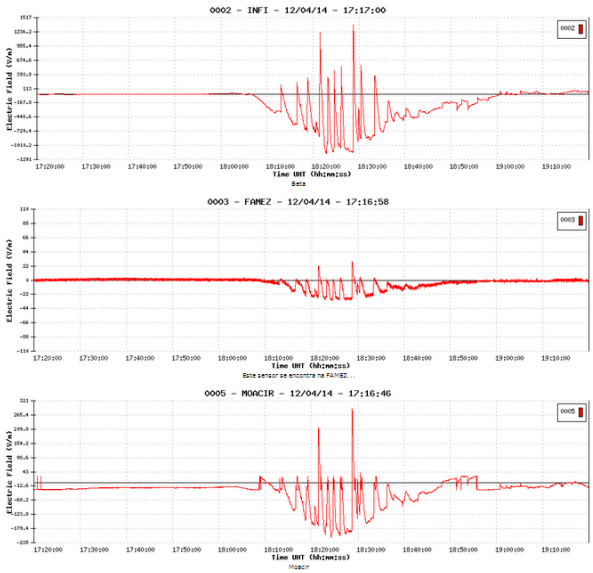

Figure 5. Electric Field measured by 3 EFMs during a thunderstorm.

4 – RESULTS

In this topic we present the analysis' results of fair weather electric field between October, 2013 and January, 2015 and the construction of a Carnegie's curve based on the duration of the thunderstorms.

4.1 ANALYSIS OF FAIR WEATHER MEASUREMENTS

The EFM data is recorded at a rate of 1 Hz. So, the file for one day has 86400 lines. The first step is to synchronize all the files, because in some of them there are lost lines. Then, the mean value is obtained for a mean-day, by summing all data for each equal second of different days and dividing for the total of numbers of the sum. The result of this sum is presented as the black curve of figure 7. The other step is to use Fourier Transform to decompose the black curve in several harmonics and their respective periods and amplitudes. These values are presented in table 1, which shows the frequencies for the 23 first harmonics, and graphically in figure 6.

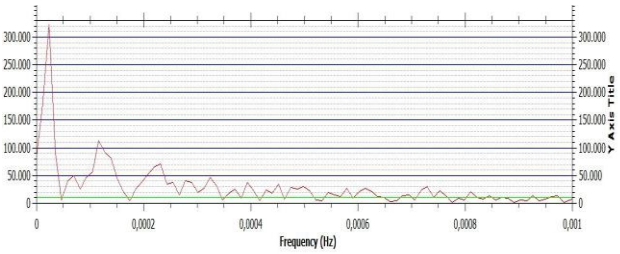

Figure 6. Fourier Transform from the black curve of figure 7 (mean-day electric field), related to Table 1.

Table 1 shows the frequencies of figure 6, obtained by using Fourier Transform to decompose the mean value of fair weather electric field to fit data (shown in figure 7).

Table 1. Fourier Transform of mean-curve of figure 7.

n	FREQUENCY (Hz)	PERIOD (s)	AMPLITUDE
1	2,31583E-05	43181,00	322645,4863
2	5,78958E-05	17272,41	40389,40478
3	6,95E-05	14393,67	50151,17913
4	0,00011579	8636,32	112441,5387
5	0,00013895	7196,83	81657,32342
6	0,00023158	4318,16	70856,87816
7	0,000254714	3925,97	38111,73606
8	0,0002779	3598,42	40129,49011
9	0,000324217	3084,36	46104,48844
10	0,000370533	2698,81	26301,6616
11	0,000393692	2540,06	37188,62288
12	0,000428429	2334,11	23772,09005
13	0,000451588	2214,41	34595,86204
14	0,000474746	2106,39	28942,71075
15	0,000497904	2008,42	30296,68925
16	0,000509483	1962,77	22186,21963
17	0,000544221	1837,49	18830,66662
18	0,000578958	1727,24	27706,20303
19	0,000613696	1629,47	26807,02254
20	0,000729488	1370,83	29612,74771
21	0,000752646	1328,65	22443,81314
22	0,000810542	1233,74	21480,3031
23	0,000926333	1079,52	13198,27151

Analyzing data of table 1, we see that there is a predominant oscillation of 12 hours (11 h 59 min 40 s). The last computed period is the 23th harmonic and it lasts18 minutes. The fit (Figure 7) was made by a sum of cosine curve weighted by their amplitudes, considering the first 21 frequencies.

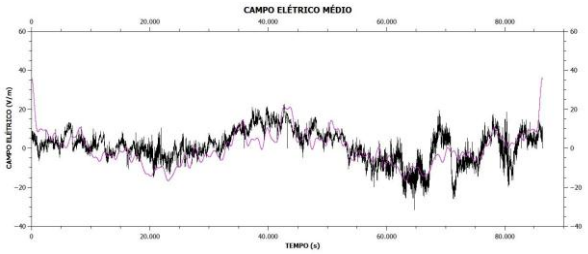

Figure 7 - Fit of fair weather measurement: mean of several months (black line) x mathematical curve (thin magenta line)

The power spectrum of harmonics is presented in Figure 8. It was obtained by using data of table one (frequency versus amplitude). The fit was made by a power curve presented inside the figure. S(f) ~ f^-0.592 and the R2 = 0.4491. For comparison, if we do not consider the most discrepant point in figure 6, the curve for S is S(f)~f^-0.617 and R2 = 0.73.

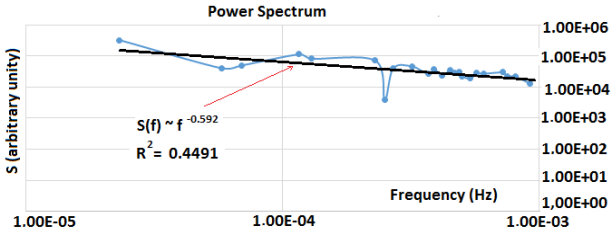

Figure 8. Frequency spectrum. Frequency in Hz versus Amplitude in arbitrary unity.

4.3 ANALYSIS OF THUNDERSTORM ACTIVITY

Table 2 shows the selected thunderstorms used in this paper to study the electric field during electrical activity. The red horizontal bars represent the beginning and the end of the selected thunderstorm.

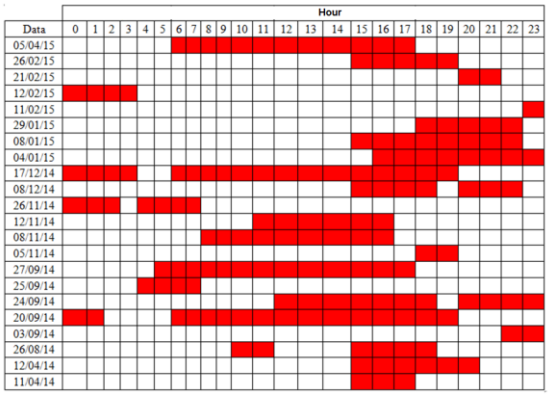

Table 2 Selected storms. The red horizontal bars represent the duration of storm.

The Figure 9 shows the number of times that thunderstorms happen (y-axis) by the hour (x-axis). The hour is Local Time (LT) (GMT= LT+4). . The curve roughly represents the Carnegie's curve showed in figure 14 with a peak around between 19:00 and 20:00 GMT.

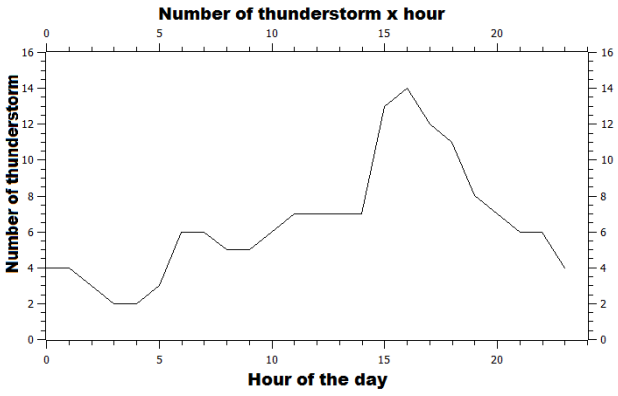

Figure 9 Representation of the number of hours with lightning activity versus hour of the day (Local Time).

Figure 10 shows a typical result of electric field measurement in real time, showing the evidences of pre-activity inside cloud and the EOS pattern with decreasing lightning activity. The colored numbered horizontal bar represents possible levels of alert. The green bar is represented by the number 1, the yellow, 2, the orange 3 and the red, 4.

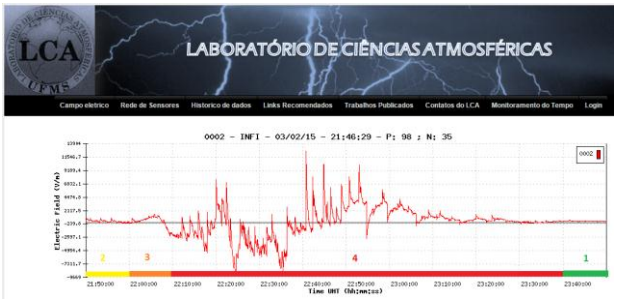

Figure 10. Level of alerts numbered by colors: 2 (yellow) medium risk, 3 (orange) high risk, 4 (red) extreme risk; 1 (green) no risk.

The level 1 is characterized by no risk; in this condition usually electric field presents oscillation but no close activity. In level 2 there are evidences of discharge due to the shape of the pulses registered and because of the electric field, it starts to grow or decrease like a hook. Level 3 the hook shape is complete and the field is strong, sometimes there are electrical discharges inside cloud, thunders can be listened. Level 4, there are cloud to ground lightnings occurring. The EOS shape is variable, but is characterized by a possible low electrical activity or restart of activity after a deactivated period, or even a gradual decrease in lightning activity. Sometimes appear oscillations during the EOS as represented in figure 12.

Another detailed example (in zoom) is showed in figure 11 where the bars are replaced by arrows with the same colors of figure 10 and 12. The EOS is not shown.

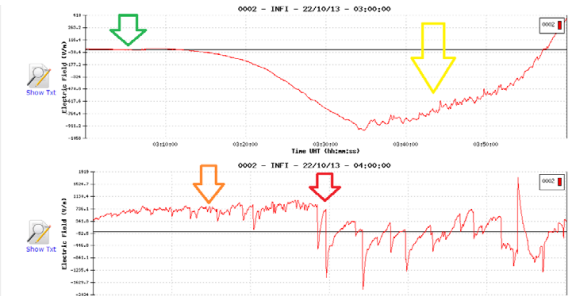

Figure 11. Typical curve for alert emission. Green arrow: no risk; Yellow arrow: attention; Orange arrow: imminent risk (high level); Red arrow: occurrence of lightning discharge to ground [11].

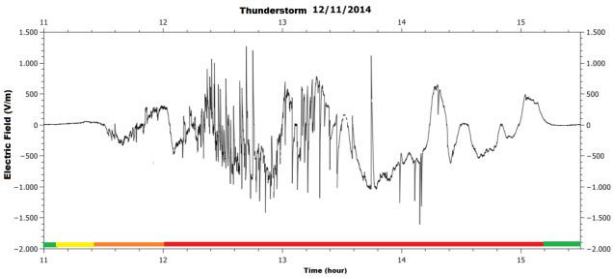

Figure 12. Thunderstorm with oscillations during EOS.

5 - ANALYSIS OF THE RESULTS

In this paper we describe some details of an EFM network installed in the city of Campo Grande, Mato Grosso do Sul, Brazil. Three results are important to analyze:

1. The behavior of fair weather electric field;
2. The Carnegie's curve obtained by using Electric Field Mill network;
3. The emission of alert of lightning risk incidence based on EFM network.

5.1 – FAIR WEATHER ELECTRIC FIELD

Direct measurements of electric field using EFM network at a height 1.5 m above ground, in a scale of time that can measure pulsations in a range from 10^{-3} to 1 Hz, were performed by Anisimov et al [4]. They found such oscillation of earth's fair weather electric field and according to them these frequencies are associated with the size of spatial scale of ions movement in the troposphere. According to these authors, both turbulent mixing of charged particles and thermal convection in surface layer could explain the nature of electric pulsation of the atmosphere.

The ranges of spatial and temporal dimensions of these pulsations were estimated to be 500 – 1000 m and times not less than 10 minutes [5]. The same author and collaborators concluded that the magnitude of these pulsations under fog conditions is intensified by a factor greater than one order of magnitude [5].

The spectra of such pulsations was measured by Anisimov et al. that proposed a mechanism that makes clear the connection of this spectra and the formation of

aero-electric structures and the “key role of the non-local relationship of the electric field and the space charge density pulsations” [6].

Direct measurements of electric field made in the ranges of frequencies between 0.004 and 0.06 Hz using a different technique were performed by Yerg and Johnson [7]. These authors used a passive cooper screen antenna 1 m above the ground and concluded that the existence of fluctuations of atmospheric electric fields are associated primarily with drifting clouds of space charge located near the level of the antenna (local turbulence or convection). The rate of electric field variation due to charges within the clouds is about one half of that one associated with drifting clouds, or about one third of the locally rate change of the potential gradient [7]. The spectrum of frequency has a peak at 0.001 Hz that means a period of about 1000 seconds [7].

To analyze the measured pulsation in the frequency range from 0.001 Hz to 1 Hz measured at about 1.5 m above the ground under fair-weather conditions, Anisimov et al constructed a structural function, D, based in two possible mechanisms that imply in variation of position of charges that produces variation in electric fields [4]. One of them occurs inside the cloud and is related to the different mobility of heavy and light ions under electric field and profiles of temperature. The other one takes place in the surface layer and is related to the turbulence that occurs due to the formation of turbulent eddies mix charged particles in this space charge, that disperses mean charge and conductivity profiles. This causes fluctuations in that range of 0.001 Hz that can be expressed in terms of neutral gas velocity pulsations [4].

In this work, the resolution of electric field measurement is greater than one volt and in most of the sensors installed on ground we didn’t detect any regular Oscillation of Electric Field (OEF). The sensor that detected it was installed 1m over the ceiling of an 8m tall building. In such conditions, even having low resolution compared with Anisimov measurements, we detected oscillations of frequency lower than 10E-3 Hz, which corresponds to periods greater than 1000 s. The strongest one has a period of 12 hours. We didn’t find any local electrical perturbation with such regularity. So, we associated these electrical oscillations to atmosphere movements in a range greater than those calculated by Anisimov and collaborators. Considering that atmospheric pressure has the same period, and the non-locality eluded by Anisimov et al [6], the first hypothesis we establish associate this oscillation to variation of atmospheric pressure. A second hypothesis is to suppose that this oscillation is due to alternating existence and nonexistence of the lower layers of ionosphere. A third hypothesis is that both processes analyzed before combine themselves to produce this oscillation.

5.2 – CARNEGIE’S CURVE

Carnegie’s curve is another evidence of non-locality of electric field variation and can be obtained by different methods [8] [9] [10] [12]. The classical method is computing the hour that occur thunders and another is counting lightning discharges that occur in an interval of time [9] [10].

In this paper we demonstrate that the use of EFM is a tool to construct Carnegie’s Curve. The technique is too simple and consists of recording the thunderstorm by date in a worksheet like that one presented in table one and then filling the matrix (see table 2) with zeros (when no lightning thunderstorm is presented) and 1 (when there is lightning activity – red horizontal bars) and finally summing the columns. We present now a preliminary result because we selected only a few thunderstorms (as we can see in Figure 15). In figure 15 (adapted from reference [9]) we plot the curves of the discharge counting in every second (blue and red curves) and the counting of hour with lightning activity (black curve). We believe that when we will compute too many thunderstorms we will reproduce more accurately the curve presented in figure 14. These processes are being automatized and we wait to improve the curve presented in figure 9 using this methodology, in a few months.

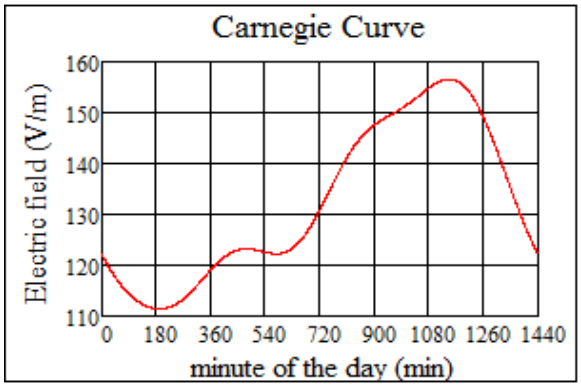

Figure 14 Carnegie’s Curve (adapted of Lacerda et al [9])
Source: Harrison [8]

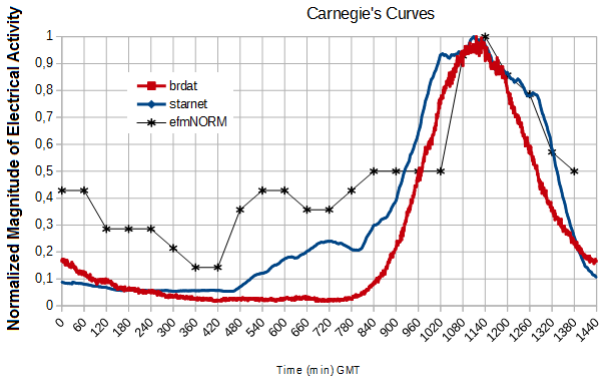

Figure 15. Comparison of Carnegie’s curve. STARNET and BRDAT are Lightning Locating Systems; efmNORM is the curve of normalized result of table 2 and figure 9. Adapted of Ref [10]. The x-axis is measured in minutes.

Notice that in figure 14, the smaller value (111) represents about 0.7 of maximum value (~156). This means that all the curve of figure 14, before the peak, is over 0.7 in figure 15. Considering preliminarily correct the black curve of the figure 15, this means that the Lightning Detection Systems are underestimating the lightning activity from 00:00 to 15:00 h GMT. More researches are necessary to understand better these differences.

5.3 EMISSION OF RISK ALERT.

According to this work there would be used two criteria for lightning risk alert: the shape of the electric field variations and a threshold of electric field. The first one is more important than the second one. While the first one allows understanding some processes that occurs inside the cloud, the second one can be used to estimate the distance from the cloud.
As we wrote in section 3.2.2, by using only a threshold there is an increase in the non-alert with close activity and the false alert without considerable risk of lightning occurrence. The first reason was presented in section 3.2.2, when we affirm that sometimes the two sensors had low values even being near activity. The second reason is that in some cases the cloud produces intense electric field, but no lightning is produced. Perhaps are occurring monopole structures or even weak bipolar structures that disappear without lightning occurrence. In these cases, the electrical field varies during falling rain but no lightning pulses are observed. In some cases, small pulses are observed. The activity inside cloud that means pre-discharge process is composed of small lightning pulses, and these variations are quite different from that produced by falling rain.

The analysis of data allows us to separate the curve of electric field in four regions. The first one (green), represents no risk region. The second (yellow), means attention, or low risk and the third (orange), means high lightning risk. Finally the fourth (red), represents extreme risk because we had registered at least one discharge cloud to ground. Comparing the duration of the second and third regions (risk 2 and 3, respectively) we could estimate that an alert can be done between 10 and 20 minutes before the falling of the first discharge.

6 - CONCLUSIONS

In this paper we describe some details of an EFM network, installed in the city of Campo Grande, Mato Grosso do Sul, Brazil. Three results are important to analyze:

1. The oscillatory behavior of fair weather electric field;

2. The Carnegie curve obtained by using Electric Field Mill;

3. The emission of alerts of lightning incidence risks based on EFM network.

The main conclusions are:

6.1 The fair weather electric field was analyzed by using Fourier Transform and allowed to detect the frequency of several harmonics. We used the first 23 harmonics to fit the data curve. The main oscillation has periods of about 12 hours. We hypothesize that these electric oscillations are produced by atmosphere movements that cause variations of pressure during the day. The second hypothesis is to suppose that this oscillation is due to alternating existence and nonexistence of the lower layers of ionosphere. A third hypothesis is that both processes analyzed before combine themselves to produce this oscillation.

6.2 Carnegie's Curve can be obtained by electric field measurements of a field mill by computing the hours in the day that field mill records thunderstorm electrical activity.

6.3 Field Mill Network may reduce the number of false alerts or no alert better than a single EFM.

6.4 The data analysis allows us to separate the electric field curve in four regions. The first one (green), represents no risk region. The second (yellow), means attention, or low risk, and the third (orange), means high lightning risk. Finally the fourth (red) represents extreme risk because we had registered at least one discharge cloud to ground.

6.5 Comparing the duration of the second and third regions (risk 2 and 3, respectively) we could estimate that an alert can be done between 10 and 20 minutes before the falling of the first discharge.

Acknowledgment: Andressa Regnold, for gramatical revision

7 – REFERENCES

[1]Jacobson, E. A., Krider, E. P., Electrostatic Field Changes Produced by Florida Lightning, Journal of Geophysics Research, p. 103, jan 1976.

[2[Koshak, W. J., Krider, E. P., Analysis Of Lightning Field Changes During Active Florida Thunderstorms, Journal of Geophysical Research,V. 94, N. D1, p.p. 1165-1186, Jan, 1989

[3] LACERDA, M. *et al*. A methodology to study charged cloud structure based on field mill networks by solving the inverse problem of Coulomb's law. Bonito: Ground'2012 & 5th LPE, 2012.

[4] Anisimov, S. V., Bakastov, S. S., Mareev, E. A., Spatiotemporal structures of electric field and space charge in the surface atmospheric layer, Journal of Geophysical Research, VOL 99, N. D5, p.p. 10603-10610, may 20, 1994.
[5] Anisimov, S. V., Mareev, E. A., ., Bakastov, S. S., On the generation and evolution of aeroelectric structures in the surface layer, Journal of Geophysical Research, VOL 104, N. D12, p.p. 14359-14367, june 27, 1999.
[6] Anisimov, S. V., Mareev, E. A., Shikhova, N. M., Dimitriev, E. M. Universal spectra of electric field pulsations in the atmosphere, Geophysical Research Letters, VOL 29, N. 24, p.p. 2217, doi:10.1029;2002GL015765, 2002.
[7] Yerg, G. D., Johnson, K. R., Short-Period Fluctuations in the Fair-Weather Electric Field , Jounal of Geophysical Research, VOL 79, N. 15, p.p. 2177-2184, may 20, 1974
[8] Harrison, R. G., The Carnegie Curve, Surveys in Geophysics 34:209-232 (2013).
[9] Lacerda, M., Jaques, R Diurnal variation of lightning activity based on data recorded by the global lightning location system STARNET., Proceedings of XIV International Conference on Atmospheric Electricity, Rio de Janeiro, Brazil, August, 2011.
[10] Lacerda, M., Jaques R., Saba, M.M.F., Campos, D. R., Nacaratto, K.P., Comparison of Carnegie's Curve for South America, XII SIPDA, International Symposium in Lightning Protection, Belo Horizonte, Brasil, 2013.
[11] UFMS NEWS, reportagem, agosto 2014.
[12] Bailey J.C.; Blakeslee R. J.; Buechler D. E.; Christian H. J.; Diurnal Lightning Distributions as Observed by the Optical Transient Detector (OTD) and the Lightning Imaging Sensor (LIS); American Geophysical Union, Fall Meeting, 2006.

Main author Name: Moacir Lacerda
Address:UFMS – INFI – Unidade V; Av. Costa e Silva sn. Cidade Universitaria 79070-900 Campo Grande- MS – Brasil
moacirlacerda@gmail.com

Phone: +55 67 99810503 E-mail: moacirlacerda@gmail.com